ACTA ET COMMENTATIONES UNIVERSITATIS TARTUENSIS DE MATHEMATICA
Volume 28, Number 1, June 2024
Available online at https://ojs.utlib.ee/index.php/ACUTM

Stiffness parameter prediction for elastic supports of non-uniform rods

Helle Hein and Ljubov Jaanuska

Abstract. The present research focuses on establishing the stiffness parameter of elastic springs placed at the ends of non-uniform rods. The governing equation for the longitudinal vibrations of the rod was solved using the Haar wavelet integration method. The calculated natural frequency parameters closely aligned with those available in the literature. The normalised values of the first ten natural frequency parameters were used in the feature vector to predict the stiffness parameter of the springs. A feedforward neural network with two hidden layers made accurate predictions when the range of each natural frequency parameter within its domain exceeded one. The insights garnered from this study contribute to the design, optimisation and assessment of diverse engineering applications.

1. Introduction

Over the past several decades, extensive research on uniform rods has been conducted. Exact solutions for longitudinal vibration of homogeneous rods can be found in [11]. A study of longitudinal vibrations of two uniform rods coupled by translational springs was conducted by Kukla et al. [6] using the Green function method. The authors derived the system's frequency equation by setting the determinant equal to zero; the determinant contained $2n$ unknown variables.

The design of modern and intricate structures necessitates the utilization of non-uniform rods. Such rods exhibit variations in the cross sectional area or material properties along the length. Due to the presence of multiple coefficients in the governing differential equation of motion, an exact analytical

Received November 17, 2023.
2020 *Mathematics Subject Classification.* 68T05, 70B10, 70E15, 70E17, 70K25.
Key words and phrases. Non-uniform rods, free vibration, Haar wavelet, backpropagation network, random forest.
https://doi.org/10.12697/ACUTM.2024.28.08
Corresponding author: ljubov.jaanuska@ut.ee

solution is possible under specific conditions involving certain cross-sectional area functions and boundary conditions. For example, Raman [13] offered general solutions that apply to rods with cross-sectional area variations described by trigonometric or exponential functions, such as $cos(x)$, $sin(x)$, $e^{(-x^2)}$. Kumar and Sujith [7] obtained exact analytical solutions for the longitudinal vibration of rods with cross-sectional area changes expressed as $A(x) = (a + bx)^n$ and $A(x) = A_0 sin^2(ax + b)$. Horgan and Chan [4] provided exact solutions for the vibrations of rods whose cross-section varied as $A(x) = A_0[1 + \alpha(x/l)]^n$ when $n = -1$, 1, 2, and $A(x) = A_0 e^{(-\alpha x/l)}$. Raj and Sujith [12] studied cross-sectional area variations of rods described by $A(x) = kx^n e^{(bx^2)}$, $A(x) = kx^n e^{(bx)}$, and $A(x) = ke^{(bx)} e^{(ne^{(mx)})}$. In a recent study, Raj and Sujith [12] solved the problem with cross-sectional area $A(x) = kx^n e^{bx^2}$ and $A(x) = kx^n e^{bx}$. Guo and Yang [2] also investigated the problem with cross-sectional area $A(x) = A_0 e^{ax+bx^2}$ using Kummer functions. Yardimoglu and Aydin [15] presented analytical solutions for longitudinal vibrations of non-uniform rods with area variations of the form $A(x) = A_0 sin^n(ax + b)$ and $A(x) = A_0 cos^n(ax + b)$. Li et al. [9] presented analytical solutions for longitudinal vibrations of non-uniform rods with concentrated masses coupled by translational springs. In their study, cross-sectional area variations were set to $A(x) = ae^{(-bx/l)}$ and $A(x) = a(1+bx)^c$. In the solutions mentioned earlier, the equation of motion was solved using Schrödinger equation, integral-equation-based method, or special functions, such as Bessel, Neumann, Legendre, Hermite and Laguerre.

Recently, the wavelet transform has gained popularity in structural health monitoring for two reasons. Firstly, the wavelets are effective in solving differential and integral equations [10]. Secondly, the wavelet transform has the capability to reveal concealed aspects of data that other techniques may overlook. Importantly, the transform does not require the analysis of entire structure [8, 3]. For instance, Hein and Feklistova [3] described and successfully applied the Haar wavelet transformation method in the vibration analysis of tapered beams.

In the field of engineering, the insights into the operational behavior of supports and rods are essential. By comprehending the natural frequencies and mode shapes, engineers can assess the dynamic behavior of rod-like structures with different boundary conditions, evaluate potential resonant frequencies, and take necessary measures to avoid undesirable vibrations that may lead to structural failure or reduced performance. Despite the variety of methods for analytical and computational analysis of non-uniform rods, no simple and fast solutions applicable to the evaluation of elastic supports have been proposed. Hereof, the objective of this research is to determine the stiffness parameters of elastic supports positioned at the ends of non-uniform rods. The approach encompasses the utilisation of the Haar wavelet

integration technique to analyse 39601 non-uniform rods. In each scenario, the stiffness parameters and the first ten natural frequency parameters are computed. The resulting dataset is then employed to train a three-layered feedforward artificial neural network (ANN). The trained predictive model is accurate in estimating the stiffness parameters of elastic supports.

2. The governing equation of free vibrations of non-uniform rods

The relevant non-uniform rod of length L, constant Young's modulus E, and constant mass density ρ is shown in Figure 1. The origin of the co-ordinate system is at the left end of the rod, so that $0 \leq x \leq L$. The cross-sectional area varies continuously with the axial coordinate x. The variation is described by the distribution function $A(x)$. If $A(x)$ is constant along the length, the rod is considered as uniform.

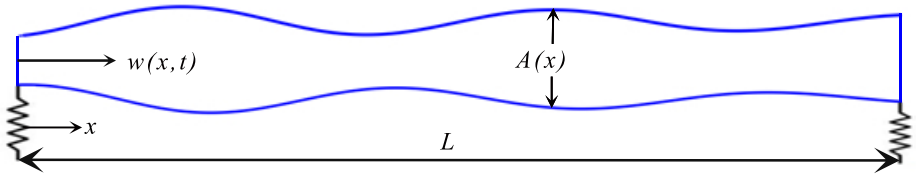

FIGURE 1. Longitudinal vibration of a non-uniform rod with an arbitrary varying cross-section.

The governing partial differential equation for the longitudinal vibration of the rod with a varying cross-section is [12]

$$\frac{\partial}{\partial x}\left[EA(x)\frac{\partial w(x,t)}{\partial x}\right] = \rho A(x)\frac{\partial^2 w(x,t)}{\partial t^2}, x \in (0,L), t \geq 0, \tag{1}$$

where $w(x,t)$ represents the axial displacement of the rod at distance x at time t. Assuming the displacement function varies harmonically with time (a solution of the form $w(x,t) = W(x)e^{i\omega t}$), equation (1) is reduced to the following ordinary differential equation:

$$\frac{d^2W(x)}{dx^2} + \frac{1}{A(x)}\frac{dA(x)}{dx}\frac{dW(x)}{dx} + k^2W(x) = 0, \tag{2}$$

where $W(x)$ represents the mode shape and

$$k^2 = \frac{\omega^2\rho}{E}, \tag{3}$$

k is the natural frequency parameter and ω is the circular frequency.

Introducing the quantities

$$\xi = \frac{x}{L}, \quad k_*^2 = k^2 L^2, \tag{4}$$

the equation of motion for the longitudinal vibrations of rods is given as

$$\frac{d^2W(\xi)}{d\xi^2} + \frac{1}{A(\xi)}\frac{dA(\xi)}{d\xi}\frac{dW(\xi)}{d\xi} + k_*^2 W(\xi) = 0, \xi \in [0,1]. \tag{5}$$

The longitudinal modal characteristics of the restrained rods can be achieved by solving the governing equation and boundary conditions simultaneously. In the case of non-uniform rods with functionally distributed cross-sectional area, the differential equation (5) has multiple coefficients; hence, an analytical solution is not available. In the present research, it is proposed to solve the differential equation with the aid of wavelets.

3. Integration of Haar wavelets

The Haar wavelet is one of the simplest wavelets which is discontinuous and resembles a step function. The Haar wavelet family for $\xi \in [0,1]$ is defined as follows:

$$h_i(\xi) = \begin{cases} 1 & \text{for } \xi \in [\xi^{(1)}, \xi^{(2)}), \\ -1 & \text{for } \xi \in [\xi^{(2)}, \xi^{(3)}), \\ 0 & \text{elsewhere,} \end{cases} \tag{6}$$

where

$$\xi^{(1)} = \tfrac{k}{m}, \xi^{(2)} = \tfrac{k+0.5}{m}, \xi^{(3)} = \tfrac{k+1}{m}. \tag{7}$$

The integer $m = 2^j (j = 0, 1, \ldots J)$ is the factor of scale; $k = 0, 1, \ldots m-1$ is the factor of delay. The integer J determines the maximal level of resolution. The index i in the system (6) is calculated as $i = m + k + 1$; the minimal value for i is one (if $j = 0$, then $m = 1, k = 0$); the maximal value of i is $2M$, which is 2^{J+1}. If $\xi \in [0,1]$ and the index i is equal to one, the corresponding scaling function is $h_1(\xi) = 1$, elsewhere $h_1(\xi) = 0$.

Hsiao and Wang [5] introduced the Haar coefficient matrix $H_{(2M\times 2M)}(i,l) = h_i(\xi_l)$. The collocation points are defined as:

$$\xi_l = \tfrac{l-0.5}{2M}, l = 1, 2, \ldots, 2M. \tag{8}$$

For the further research, the integrals of the wavelets are required

$$p_{\alpha,i}(\xi) = \textstyle\int_0^\xi p_{\alpha_{i-1,i}(\xi)} d\xi, \tag{9}$$

where α is the order of integration, i is the number of the wavelet. In (9), $p_{0,i}(\xi) = h_i(\xi)$. These integrals were calculated analytically by Lepik [8]. In

the case of $i = 1$, the integral of the wavelet is $p_{\alpha,1}(\xi) = \xi^{\alpha}/\alpha!$. In the case of $i > 1$, the integral of the wavelet is

$$p_{\alpha,i}(\xi) = \begin{cases} 0 \quad \text{for} \quad \xi < \xi^{(1)}\,, \\ \\ \frac{1}{\alpha!}(\xi - \frac{k}{m})^{\alpha} \quad \text{for} \quad \xi \in [\xi^{(1)}, \xi^{(2)}]\,, \\ \\ \frac{1}{\alpha!}[(\xi - \frac{k}{m})^{\alpha} - 2(\xi - \xi^{(2)})^{\alpha})] \quad \text{for} \quad \xi \in [\xi^{(2)}, \xi^{(3)}]\,, \\ \\ \frac{1}{\alpha!}[(\xi - \frac{k}{m})^{\alpha} - 2(\xi - \xi^{(2)})^{\alpha} + (\xi - \xi^{(3)})^{\alpha}] \quad \text{for} \quad \xi > \xi^{(3)}. \end{cases} \tag{10}$$

The values $p_{\alpha,i}(0)$ and $p_{\alpha,i}(1)$ should be calculated in order to satisfy the boundary conditions. Evaluating integrals (10) in the collocation points, the following form could be obtained:

$$P^{(\alpha)}(i,l) = p_{\alpha,i}(\xi_l), \tag{11}$$

where $P^{(\alpha)}$ is a $2M \times 2M$ matrix. It should be noted that the computation of the matrices $H(i,l)$ and $P^{(\alpha)}(i,l)$ is carried out only once.

4. General solution in terms of the Haar wavelet integration

According to Lepik [8], Hsiao and Wang [5], the highest-order derivative can be expanded into the Haar series instead of solving the differential equation. In the present study, it is assumed that the second derivative of the solution (2) is sought in the following form:

$$W''(\xi) = \sum_{i=1}^{2M} a_i h_i(\xi), \tag{12}$$

where a_i are the unknown wavelet coefficients. Integrating (12) two times and taking into account (9) and (10), the following equations are obtained:

$$W'(\xi) = \sum_{i=1}^{2M} a_i p_{1,i}(\xi) + W'(0), \tag{13}$$

$$W(\xi) = \sum_{i=1}^{2M} a_i p_{2,i}(\xi) + W'(0)\xi + W(0). \tag{14}$$

The quantities $W(0)$ and $W'(0)$ can be evaluated from the boundary conditions. If the rod is rigid at the left end $\xi = 0$ and free at the right end $\xi = 1$ of the rod, the boundary conditions are

$$W(0) = W'(1) = 0. \tag{15}$$

If the ends of the rod are free, the boundary conditions are

$$W'(0) = W'(1) = 0. \tag{16}$$

If the rod is fixed at both ends, the boundary conditions are

$$W(0) = W(1) = 0. \tag{17}$$

For the elastically constrained ends, the following boundary conditions are considered:

$$S_L W(0) - \left.\frac{dW(\xi)}{d\xi}\right|_{\xi=0} = 0, \tag{18}$$

$$S_R W(1) + \left.\frac{dW(\xi)}{d\xi}\right|_{\xi=1} = 0, \tag{19}$$

where S_L and S_R are the boundary restraining stiffness parameters on the left and right ends of the rod, respectively.

5. Numerical results

The described theoretical formulation of the Haar wavelet integration and the differential equation for the vibrations of non-uniform rods with elastic constraints was implemented in the MATLAB environment. Two numerical examples were examined.

5.1. A rod with cross-sectional area variation of $A(x) = A_0(ax+b)^n$. In the first numerical example, a non-uniform rod with elastically restrained ends and a cross-sectional area variation of $A(x) = A_0(ax+b)^n$ was considered. The parameters were fixed to $a = 2$, $b = 1$, $n = 2$. The stiffness parameters of the springs on the left and right sides of the rod $S_L = Lk_L/EA(0)$ and $S_R = Lk_R/EA(1)$ varied in the range $[10, 20, ..., 1990]$. In total, 39601 cases were calculated numerically when the level of resolution of the Haar wavelets was set to five ($J = 5$). For each case, the first ten natural frequency parameters were calculated. The results were compared with the ones available in the literature: the first frequencies were in excellent agreement with the results published by Xu et al. [14] (Table 1).

TABLE 1. Non-dimensional natural frequencies of elastically restrained non-uniform rods with cross-sectional area variation of $A(x) = A_0(ax+b)^n$, $a = 2$, $b = 1$ and $n = 2$.

S_L	S_R	f_1 [14]	f_1
10	10	1.6884	1.6883
100	100	2.8476	2.8473
1000	1000	3.1104	3.1102

To construct, train and evaluate an ANN, the dataset was divided into two sets: the training set of 33661 records (85%) and the independent test set of 5940 records (15%).

After multiple manipulations with the structure of the ANN (the number of layers, hidden neurons, optimisation algorithm), it was observed that the most promising network had three layers: the input layer, a hidden layer with 30 neurons and a hidden layer with 15 neurons. The learning process was carried out by Broyden–Fletcher–Goldfarb–Shanno optimisation algorithm (*trainbfg*). To train the network, the feature vector contained the normalised values of the first ten natural frequency parameters. The performance of the model was evaluated on the independent test set: root mean squared error ($RMSE$) was 41.6601, mean absolute error (MAE) was 30.5982, coefficient of determination (R^2) was 0.9947, normalised mean squared error ($NRMSE$) was 0.0013 and Pearson correlation coefficient (R) was 0.9974. The predicted values against the actual values and the error histogram are plotted in Figure 2: a) the x-axis is labeled with the record number of the test; b) the x-axis is labeled with the first natural frequency parameter (the parameter varies in the range between 1.6883 and 3.1257).

The predicting accuracy of the ANN was slightly improved when the feature vector contained the stiffness parameter of the second spring and the normalised values of the first three natural frequency parameters: $RMSE = 28.8038$, $MAE = 19.2414$, $R^2 = 0.9988$, $NRMSE = 0.0006$ and $R = 0.9988$. The predicted values against the actual and the error histogram are visualised in Figure 3. It is important to note that if the feature vector comprised all ten normalised natural frequency parameters along with the stiffness parameter of the second spring, the model's ability to accurately predict the stiffness parameter of the spring on the left side of the rod decreased.

5.2. A rod with cross-sectional variation of $A(x) = A_0 sin^n(cx + d)$.

In the second numerical example, a rod with elastically restrained ends and a cross-sectional area variations given by $A(x) = A_0 sin^n(cx + d)$ was considered. The parameters were fixed to $c = 2$, $d = 1$ and $n = 2$. The stiffness parameters of the springs on the left and right sides of the rod varied in the range $[10, 20, ..., 1990]$. In total, 39601 cases were calculated numerically when the level of resolution of the Haar wavelets was set to five ($J = 5$). For each case, the first ten natural frequency parameters were calculated. The results in the the case of $S_L = 0$ and $S_R = 1$ were in excellent agreement with results presented by Yardimoglu and Aydin [15].

Applying the procedure described in Subsection 5.1, the predicting accuracy of the three-layered ANN trained on the normalised values of the first ten natural frequency parameters was $RMSE = 132.8334$, $MAE = 69.6468$, $R^2 = 0.9464$, $NRMSE = 0.0132$ and $R = 0.9728$. The predicted values against the actual and the error histogram are visualised in Figure 4.

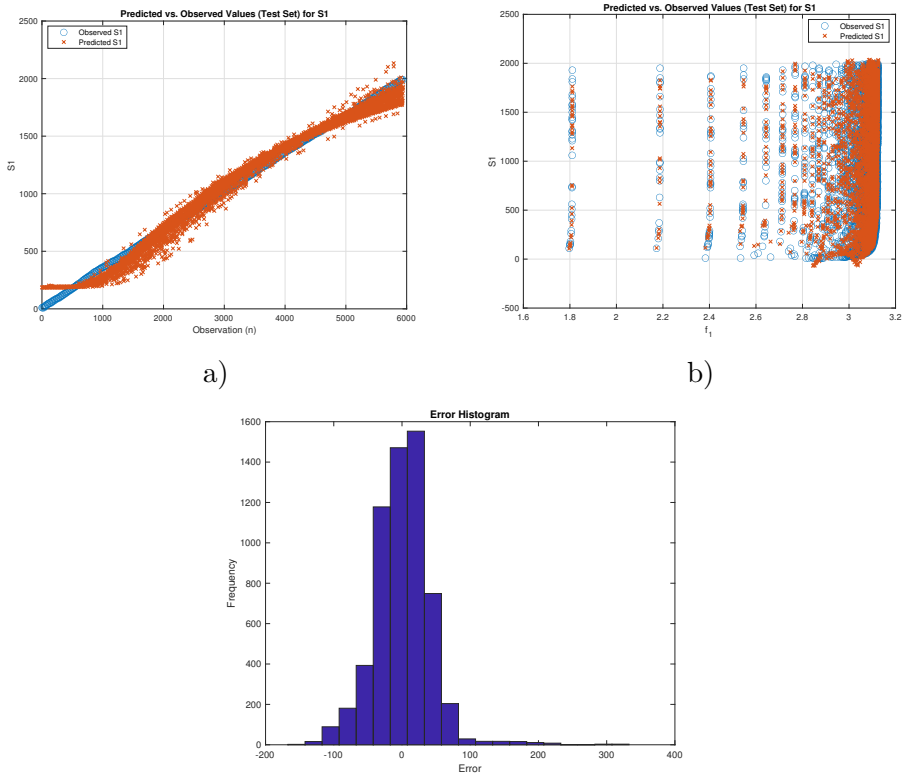

FIGURE 2. Stiffness parameter prediction using the normalised values of the first ten natural frequency parameters: a), b) - predicted values against actual values, c) - error histogram.

TABLE 2. Non-dimensional natural frequencies of elastically restrained non-uniform rods with cross-sectional area variation of $A(x) = A_0 sin^n(cx + d)$, $c = 2$, $d = 1$ and $n = 2$.

S_L	S_R	f_1	f_2	f_3	f_4	f_5	f_6
0[a]	1	2.14856	5.535762	8.632811	11.694641	14.757858	17.830596
0	1	2.14847	5.535737	8.633668	11.698285	14.767315	17.849956

[a] The results in the row were obtained by Yardimoglu and Aydin [15].

The poor performance of the network can be attributed to the low variance of the features in their domain (Figure 4 b, Table 3).

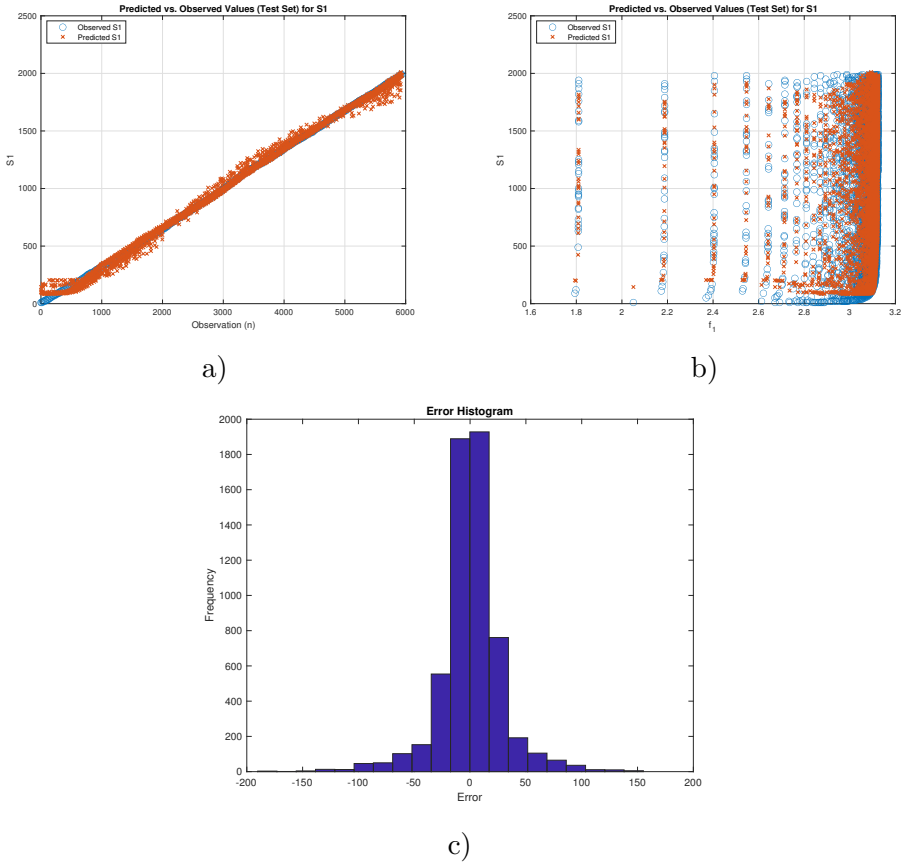

FIGURE 3. Stiffness parameter prediction of the spring at the left end of the rod using the normalised values of the first three natural frequency parameters and the stiffness parameter of the spring at the right end of the rod.

TABLE 3. The minimum and maximum values of the first eight natural frequency parameters.

f_1	f_2	f_3	f_4	f_5	f_6	f_7	f_8
2.1614	5.5528	8.65223	11.71438	14.7778	17.8528	20.94207	24.0460
2.4180	5.9496	9.2026	12.4005	15.5801	18.7533	21.9260	25.1012

The predicting accuracy of the ANN was improved when the feature vector contained the stiffness parameter of the second spring and the normalised values of the first three natural frequency parameters: $RMSE = 15.2222$, $MAE = 6.9012$, $R^2 = 0.9993$, $NRMSE = 0.0002$ and $R = 0.9997$. The

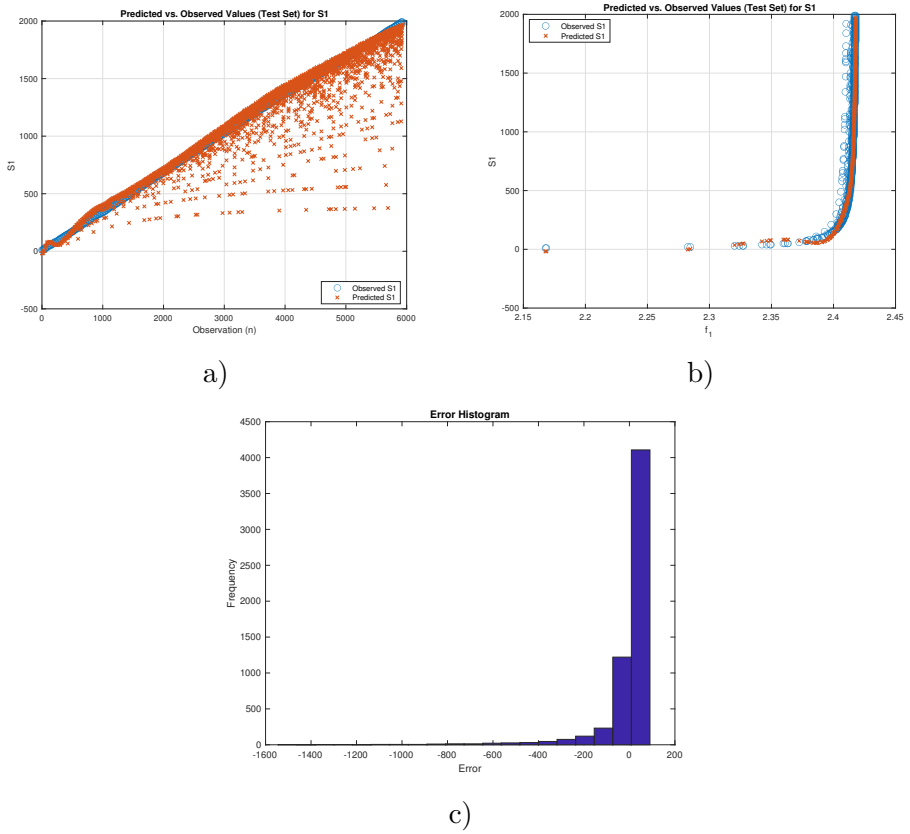

FIGURE 4. Stiffness parameter prediction using the normalised values of the first ten natural frequency parameters (a, b - predicted values against actual values, c - error histogram).

predicted values against the actual and the error histogram are plotted in Figure 5.

Discussion and conclusion

The non-uniform rods with elastic supports at the ends were considered in the present research. Two datasets were calculated applying the Haar wavelet integration method for the cases $A(x) = A_0(ax + b)^n$ and $A(x) = A_0 sin^n(cx + d)$. Each dataset contained 39601 records. The datasets were divided into the training and test sets in the ratio of 85% and 15%. A three-layered ANN could easily predict the stiffness parameter of the first spring if the range of each natural frequency parameter within its domain was greater than one. If the range was smaller than one, adding the stiffness parameter

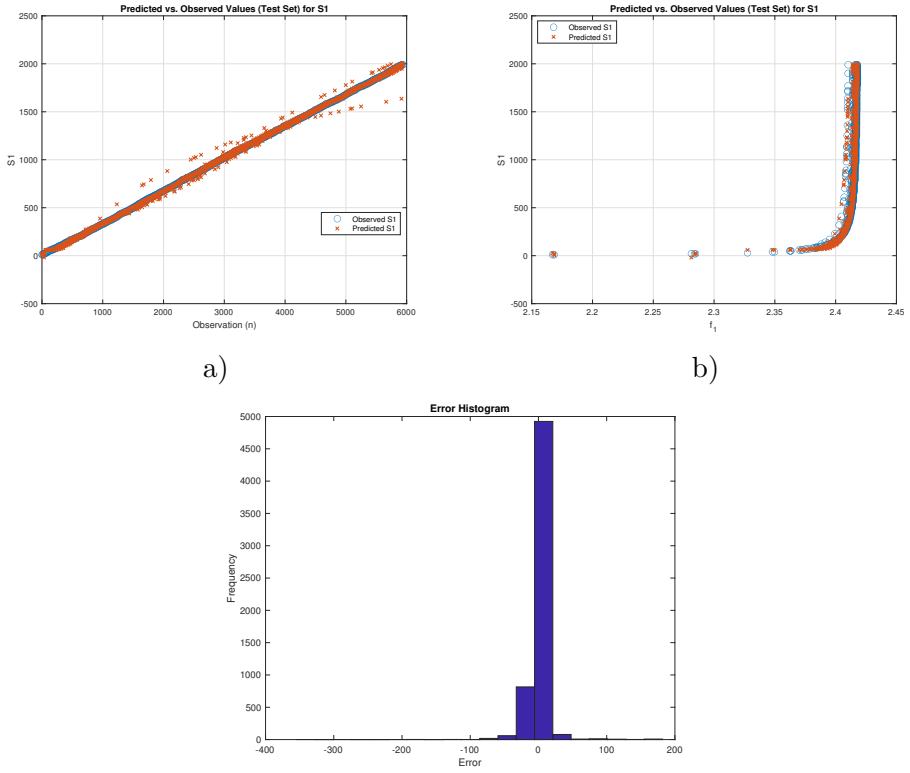

a) b)

c)

FIGURE 5. Stiffness parameter prediction of the spring at the left end of the rod using the normalised values of the first three natural frequency parameters and the stiffness parameter of the spring at the right end of the rod.

of the second elastic support as an extra feature was necessary; though, the number of the normalised natural frequency parameters could be reduced to three. The insights obtained from this study contribute to the design, optimisation and assessment of diverse engineering constructions, such as bridges, towers, shafts, and earthing systems.

References

[1] I. Elishakoff, *Eigenvalues of Inhomogenous Structures: Unusual Closed-Form Solutions*, CRC Press, Boca Raton, 2005.

[2] S. Q. Guo and S. P. Yang *Free longitudinal vibrations of non-uniform rods*, Sci. China Inf. Sci. **54** (2012), 2735–2745.

[3] H. Hein and L. Feklistova, *Free vibrations of non-uniform and axially functionally graded beams using Haar wavelets*, Eng. Struct. **33** (2011), 3696–3701. DOI

[4] C. O. Horgan and A M. Chan, *Vibration of inhomogeneous strings, rods and membranes*, J. Sound Vib. **225** (1999), 503–513. DOI
[5] C. H. Hsiao and W. J. Wang, *State analysis of time-varying singular nonlinear systems via Haar wavelets*, Math. Comput. Simulation **51** (1999), 91–100. DOI
[6] S. Kukla and others, *Longitudinal vibration of rods coupled by translational springs*, J. Sound Vib. **185** (1995), 717–722.
[7] B. M. Kumar and R. I. Sujith, *Exact solutions for the longitudinal vibration of non-uniform rods*, J. Sound Vib. **207** (1997), 721–729. DOI
[8] Ü. Lepik, *Numerical solution of differential equations using Haar wavelets*, Math. Comput. Simulation **68** (2005), 127–143. DOI
[9] Q. S. Li, G. Q. Li, and D. K. Liu, *Exact solutions for longitudinal vibration of rods coupled by translational springs*, Int. J. Mech. Sci. **42** (2000), 1135–1152. DOI
[10] J. Majak and others, *Higher-order Haar wavelet method for vibration analysis of nanobeams*, Mater. Today Commun. **25** (2020), 1577–1590. DOI
[11] L. Meirovitch, *Elements of Vibration Analysis*, McGraw-Hill, New York, 1975.
[12] R. Raj and R. I. Sujith, *Closed-form solutions for the free longitudinal vibration of inhomogeneous rods*, J. Sound Vib. **283** (2005), 1015–1030. DOI
[13] V. M. Raman, *On analytical solutions of vibrations of rods with variable cross sections*, Appl. Math. Model. **7** (1983), 356–361. DOI
[14] D. Xu, J. Du, and Z. Liu, *An accurate and efficient series solution for the longitudinal vibration of elastically restrained rods with arbitrarily variable cross sections*, J. Low Freq. Noise Vib. **38** (2019), 403–414. DOI
[15] B. Yardimoglu and L. Aydin, *Exact longitudinal vibration characteristics of rods with variable cross-sections*, Shock Vib. **18** (2011), 555–562. DOI

Department of Computer Science, University of Tartu, Estonia
E-mail address: helle.hein@ut.ee
E-mail address: ljubov.jaanuska@ut.ee